ELSEVIER

PII: S0032-3861(96)00712-4

Polymer Vol. 38 No. 8, pp. 1923–1928, 1997

0032-3861/97/$17.00 + 0.00

Melting, reaction and recrystallization in a reactive PC–PBT blend

A. N. Wilkinson* and S. B. Tattum
Department of Materials Technology, Manchester Metropolitan University, John Dalton Building, Manchester M1 5GD, UK

and A. J. Ryan
Manchester Materials Science Centre, University of Manchester and UMIST, Grosvenor Street, Manchester M1 7HS, UK and CLRC Daresbury Laboratory, Warrington, WA4 4AD, UK
(Received 22 March 1996; revised 25 June 1996)

The crystallization behaviour of PBT and a 50/50 polycarbonate (PC)–poly(butylene terephthalate) blend with added transesterification catalyst were studied using differential scanning calorimetry (d.s.c.) and synchrotron small angle X-ray scattering (SAXS)/wide angle X-ray scattering (WAXS)/d.s.c. PBT crystallization was inhibited in the blend by both the presence of PC and transesterification. Increasing transesterification resulted in a progressive reduction in the melting and crystallization temperatures and degree of crystallinity, with the development of a mixed-phase glass transition at around 90°C. Transesterification also induced a significant change in blend morphology, from a coarse (5–10 μm) bicontinuous structure, when uncatalysed, to a sub-micron bicontinuous structure at low degrees of reaction.

(Keywords: synchrotron SAXS; WAXS; reaction blends)

INTRODUCTION

Blends of polycarbonate (PC) and poly(butylene terephthalate) (PBT) have been widely studied in recent years[1–13], but conflicting conclusions have been drawn regarding their state of miscibility. This lack of agreement results from the complex melt behaviour of PC-PBT blends, in which transesterification reactions between the homopolymers, liquid–liquid phase separation and crystallization of the PBT may occur. However, a recent time-resolved light scattering study[11] unequivocally showed a 50/50 PC–PBT blend to exhibit lower critical solution temperature (LCST) type phase behaviour with a spinodal temperature (T_s) of 198°C. Thus, once a PC–PBT blend cools below T_s it will begin to phase mix and form a homogeneous mixture. However, phase dissolution, which is not a rapid process[14,15], is in kinetic competition with crystallization of the PBT which will initiate at temperatures below T_m (~220°C). PBT has one of the highest rates of crystallization of common polymers[16] and, despite some retardation due to the presence of phase-mixed PC, crystallization of the PBT-rich phase is still relatively rapid in most PC–PBT blends[10,13]. Thus, structure development within these materials tends to be dominated by PBT crystallization[5,6,8,13], which prevents significant phase dissolution and 'locks in' the biphasic morphology developed during melt blending[5,6,8,12,13]. The size-scale of this biphasic morphology decreases significantly upon the advent of interfacial transesterification between the homopolymers[12], due to the formation of AB-copolymers[2,9], which act to reduce interfacial tension in the melt. In addition, the propensity of PBT to crystallize is reduced via extensive transesterification, until eventually the blend is transformed into an amorphous, homogeneous mixture[2,9,12] comprising homopolymers and various $(AB)_n$ multiblock copolymers. In this paper, the results of simultaneous small angle X-ray scattering (SAXS)/wide angle X-ray scattering (WAXS)/differential scanning calorimetry (d.s.c.) studies of crystallization during thermal cycling of a reactive PV–PBT blend are presented, and the effects of transesterification on structure development are outlined and discussed.

* To whom correspondence should be addressed

EXPERIMENTAL

A 50/50 w/w blend of PC (Makrolon 2405, ex. Bayer) and PBT (Pocan B1505, ex. Bayer) was prepared by melt blending in a Brabender PL2000 plasticorder fitted with a W50 mixing chamber. Rotor speed, mixing time, chamber temperature and fill ratio were maintained, respectively, at 75 rpm, 2 min, 230°C and 0.8 (based on measured melt density). Transesterification was promoted by incorporating an alkyl titanium catalyst (tetrakis(2-ethyl-hexyl)titanate, Tyzor TOT, ex. Du Pont), the addition level of which was calculated to give 200 ppm titanium in the blend, based on the percentage of titanium in TOT. Organic titanates are efficient transesterification catalysts[17], widely used for the

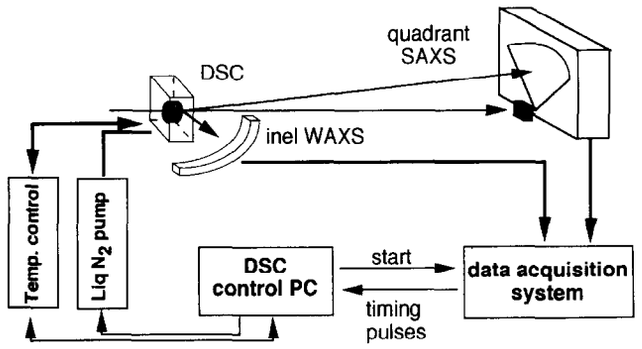

Figure 1 Experimental set up for simultaneous SAXS/WAXS/d.s.c. on beamline 8.2 of the SRS at the CLRC Daresbury laboratory

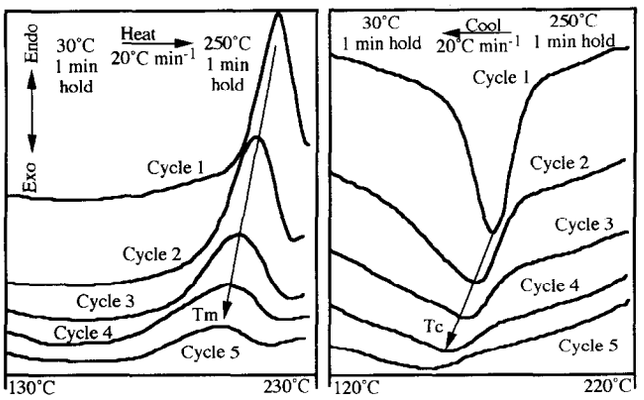

Figure 2 D.s.c. heating and cooling curves for a catalysed (200 ppm) 50/50 PC–PBT blend

manufacture of PBT[16], which also promote melt transesterification between PC and PBT[2,9,12]. A Cambridge stereoscan 250 scanning electron microscope (SEM) was used to obtain micrographs of blend structures. Samples for SEM were first cryo-fractured from liquid nitrogen, then the fracture surfaces were placed in dichloromethane (a good solvent for PC) for 1 h at room temperature, dried, and coated with gold/palladium alloy. D.s.c. measurements were made using a Perkin Elmer DSC7, calibrated using indium and zinc standards. Samples (5 mg), were encapsulated in aluminium pans and heated between 50 and 250°C at 20°C min^{-1} under flowing nitrogen, with an empty sample pan as an inert reference. To provide more information on the changes occurring within the blend as transesterification proceeds, simultaneous SAXS/WAXS/d.s.c. measurements were made on beamline 8.2 of the SRS at the CLRC Daresbury laboratory, the experimental set-up for which, shown schematically in *Figure 1*, has been described in detail elsewhere[18]. Specimens of PBT and the blend were prepared for SAXS–WAXS by encapsulating a thin slice of material ($\approx$ 0.5 mm thick) in a d.s.c. pan fitted with mica windows. The pan was inserted into a Linkam d.s.c. apparatus of the single-pan design that has been described in detail elsewhere[19]. Specimens were heated and cooled at 20°C min^{-1} between 30 and 250°C, with a 1 min hold period at the maximum and minimum temperature.

RESULTS AND DISCUSSION

Differential scanning calorimetry

The blend exhibited significant decreases in the endothermic (crystalline melting, T_m) and exothermic (crystallization, T_c) peak temperatures and the degree of crystallinity (as indicated by the peak areas) upon thermal cycling between 30 and 250°C (*Figure 2*). This behaviour may be attributed to an increase in the degree of tranesterification, producing significant quantities of statistical and short random-block copolymers, which inhibit crystallization. The blend showed no discernible glass transition until the final (fifth) heating cycle, in

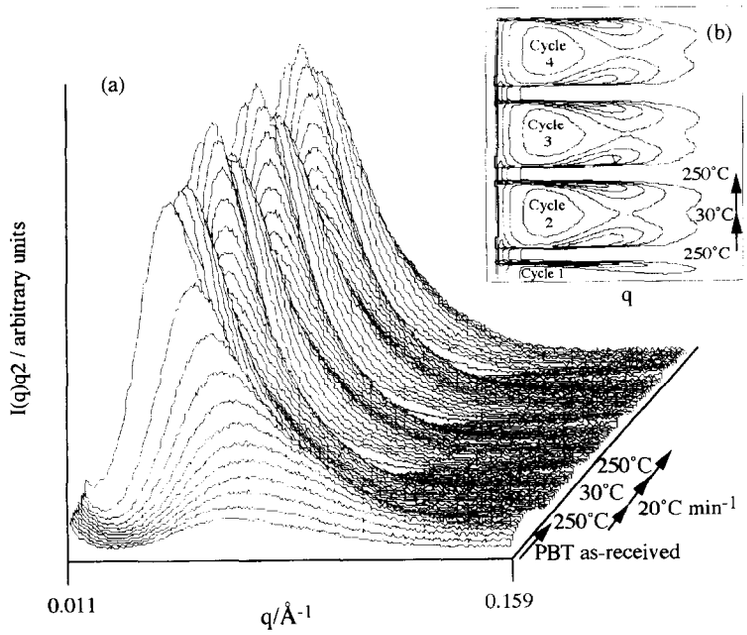

Figure 3 Three-dimensional relief diagram and the corresponding contour plot of time-resolved SAXS data during melting and recrystallization of PBT over four thermal cycles 30–250–30°C at a ramp rate of 20°C min^{-1}. For ease of interpretation the time axis has been converted into temperature, to give plots of Lorentz-corrected intensity $I(q,t)q^2$ vs scattering vector, q, vs temperature, T

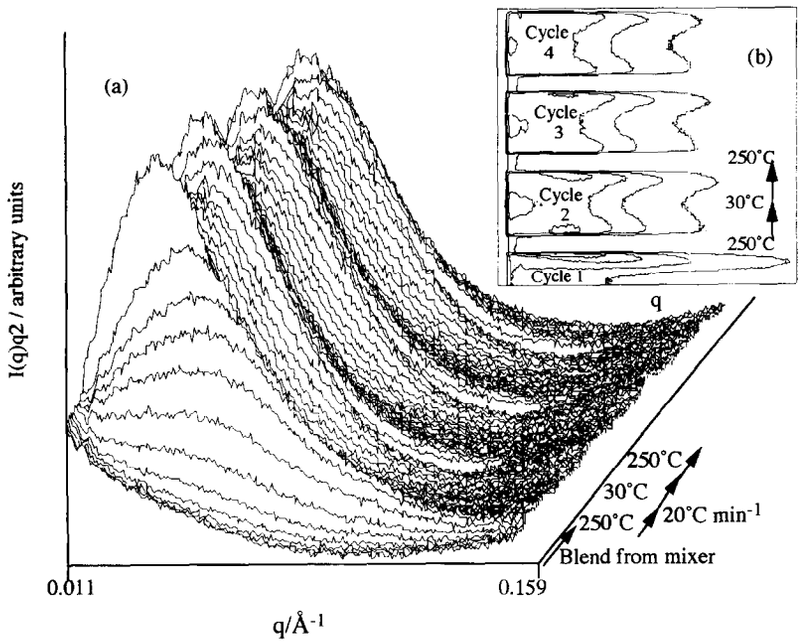

Figure 4 Three-dimensional relief diagram and the corresponding contour plot of time-resolved SAXS data ($I(q,t)q^2$ vs scattering vector, q, vs temperature, T), during melting and recrystallization of a 50/50 PC–PBT blend over four thermal cycles

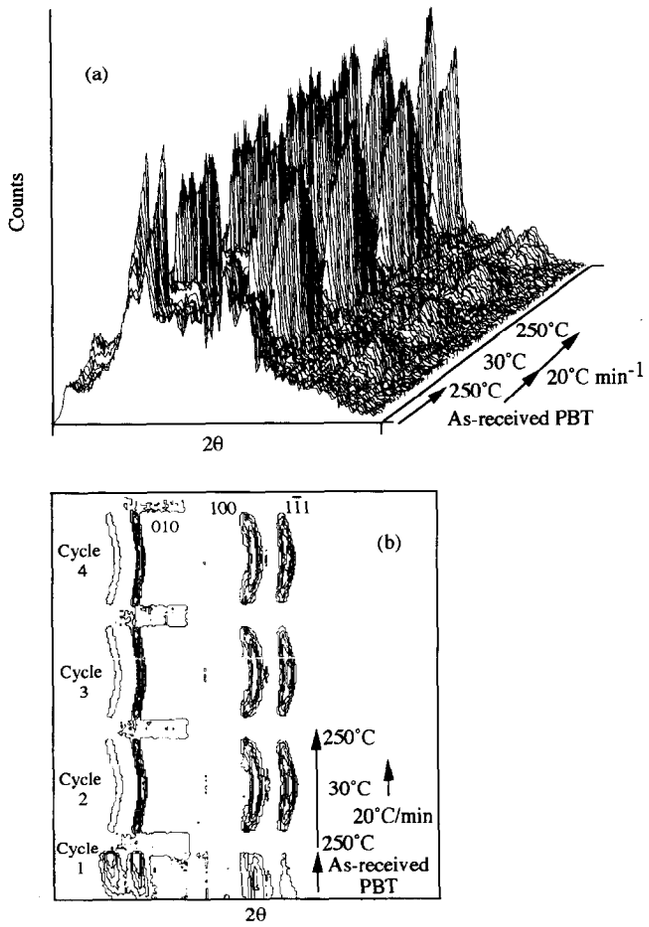

Figure 5 Three-dimensional relief diagram and the corresponding contour plot of time-resolved WAXS data ($I(2\theta,t)$ vs scattering angle, 2θ, vs temperature, T) during melting and recrystallization of PBT over four thermal cycles. The contour plot is labelled with the 010, 100 and 1$\bar{1}$1 reflections of the triclinic PBT crystals

which a broad, shallow endothermic baseline shift beginning at ~90°C was evident. This value for the glass transition temperature (T_g) agrees well with the value of 86°C predicted by the Fox equation for a homogeneous 50/50 PC–PBT material[12].

SAXS/WAXS

The SAXS data, obtained during thermal cycling of PBT and the 50/50 blend, are illustrated as three-dimensional plots and corresponding contour plots in *Figures 3* and *4*, respectively. Plots of Lorentz-corrected SAXS intensity $I(q,t)q^2$ vs scattering vector (q) vs time (t) are shown in *Figures 3a* and *4a*, respectively, and the corresponding intensity contours in *Figures 3b* and *4b*, respectively. Similarly, the WAXS data of PBT and the 50/50 blend are illustrated as three-dimensional plots of the WAXS intensity $i(2\theta,t)$ vs scattering angle (2θ) vs t in *Figures 5a* and *6a*, with the corresponding intensity contours in *Figures 5b* and *6b*. In each case, in *Figures 3–6*, the time axis has been labelled in terms of temperature.

The SAXS and WAXS data for PBT (*Figures 3* and *5*, respectively) show four thermal cycles over the experimental range 30–250°C. The first cycle removes the thermal history of the as-received PBT and produces a homogeneous melt at 250°C. Over the three cycles which follow, the PBT exhibits excellent reproducibility throughout the crystallization and melting processes, with no discernible degradation. The SAXS data illustrate the morphological complexity of the recrystallization and melting processes. Thus, during the early stages of recrystallization (200–140°C) the SAXS intensity increases rapidly then drops slightly (140–30°C), whilst throughout the temperature interval 200–30°C, the peak position (designated q^*) moves to larger values of q, that is, smaller long-spacings. The phenomena accounting for this change in q^* are due to the fractionation processes that occur during crystallization[20] which result in the formation of progressively thinner lamellae as the melt is cooled below T_c. The

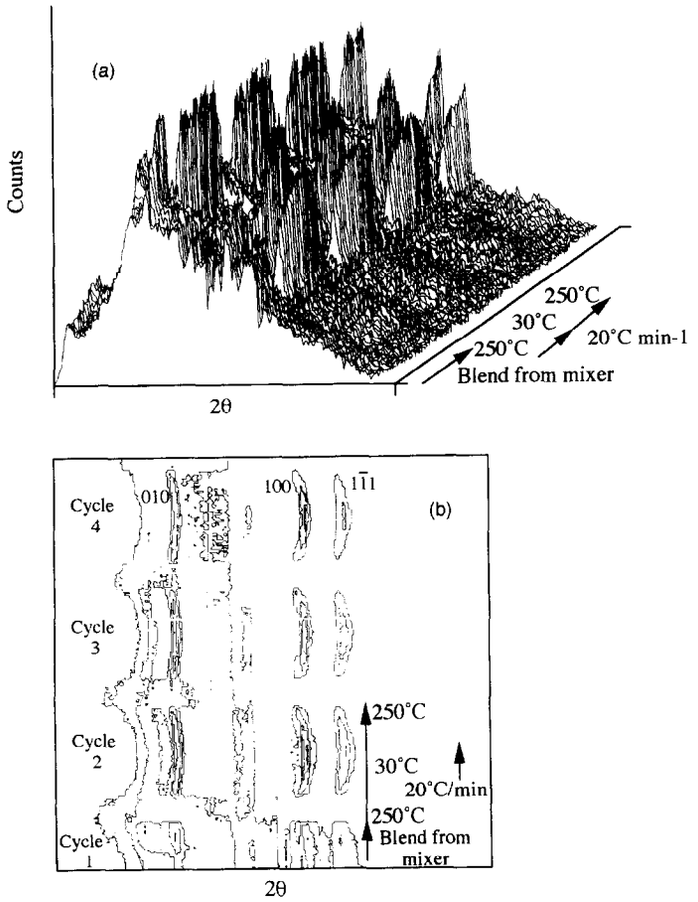

Figure 6 Three-dimensional relief diagram and the corresponding contour plot of time-resolved WAXS data ($I(2\theta, t)$ vs scattering angle, 2θ, vs temperature, T) during melting and recrystallization of a 50/50 PC–PBT blend over four thermal cycles

three-dimensional WAXS data show the variations in the intensities of the sharp 010, 100 and 1$\bar{1}$1 reflections of the triclinic PBT crystals which occur during the thermal cycles due to melting and recrystallization.

The SAXS and WAXS data for the blend (*Figures 4* and *6*, respectively) again show four thermal cycles over the experimental range 30–250°C, with the first cycle removing the thermal history of the melt blending process. Compared to the data for pure PBT (*Figure 3*), the SAXS profiles for the blend (*Figure 4*) exhibit lower intensity maxima at smaller values of q^*. This is shown more clearly in *Figure 7*, which is a plot of Lorentz-corrected intensity *versus* scattering vector for both the PBT and the blend at the same temperature (~160°C) during the second cycle. The scattering peak for the blend can be seen to be much broader ($\Delta q/q^* \approx 2$, Δq = peak width at half maximum peak height) and more shallow than the peak for PBT ($\Delta q/q^* \approx 1.5$). The interdomain spacings (d) of the PBT and the blend were calculated from the scattering maxima using Bragg's law ($d = 2\pi/q^*$) to give long-spacing values of d (PBT) ≈ 157 Å and d (blend) ≈ 209 Å. In contrast to the pure PBT, *Figure 4* (cycle 2) shows the peak position in the blend to be relatively static in the later stages of crystallization, indicating that the presence of PC has significantly retarded crystallization at lower temperatures (<160°C). In addition, during cycles 3 and 4 transesterification inhibits crystallization further, with the SAXS peak intensities (*Figure 4*) showing marked decreases. Compared to the data for pure PBT (*Figure 5*) the three-dimensional WAXS data for the blend (*Figure 6*) show

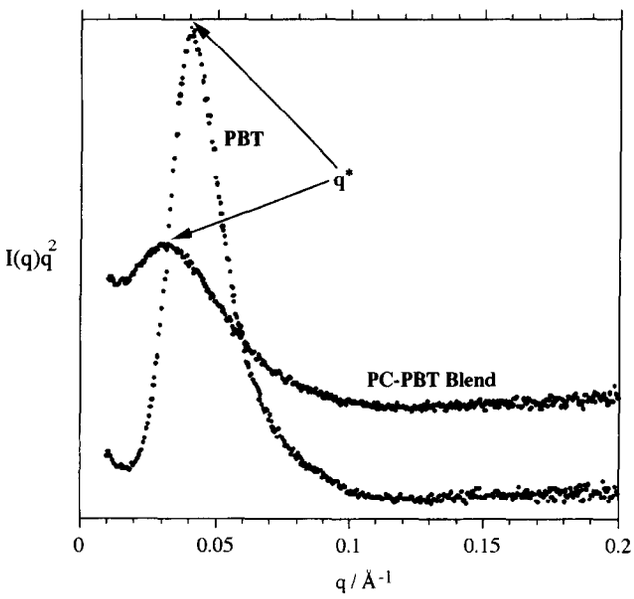

Figure 7 Lorentz-corrected intensity *versus* scattering vector for both the pure PBT and the 50/50 PC–PBT blend at the same temperature (~160°C) during the second cycle

reduced peak intensities during cycle 2, which then decrease further during cycles 3 and 4 due to transesterification.

The scattered intensity from SAXS can be related to the degree of crystallization via the relative invariant, Q', which is linear in the electron density difference $\langle \eta^2 \rangle$

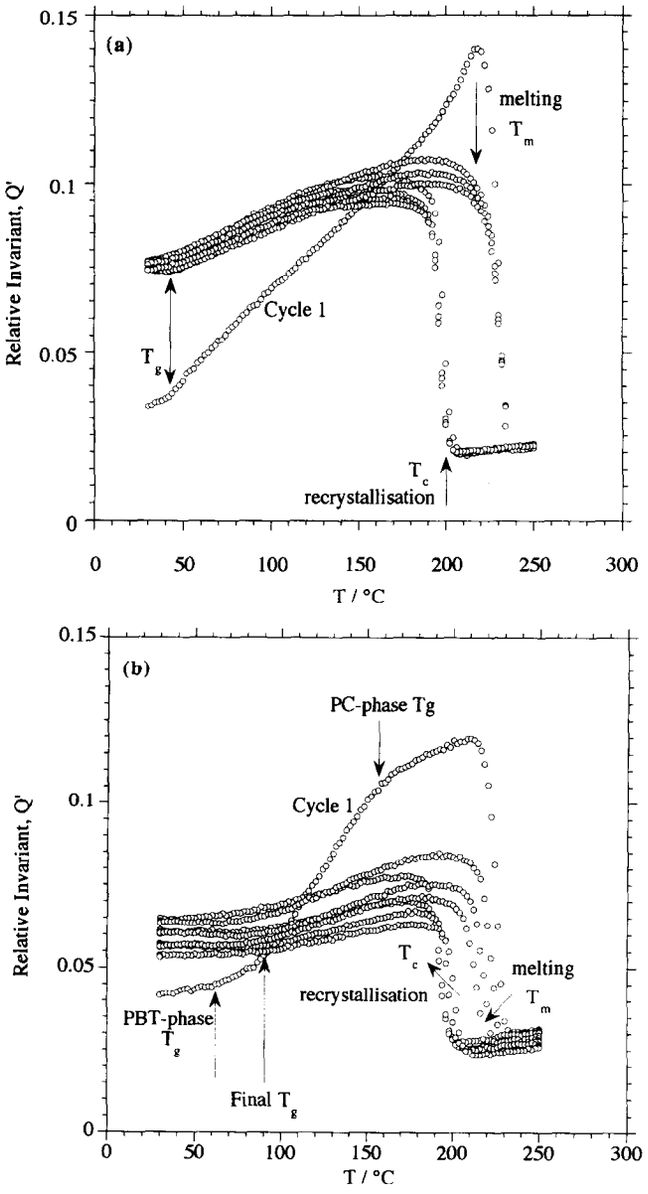

Figure 8 Temperature-dependence of the SAXS invariant, Q', during melting and recrystallization over four thermal cycles for (a) the pure PBT, and (b) the 50/50 PC–PBT blend

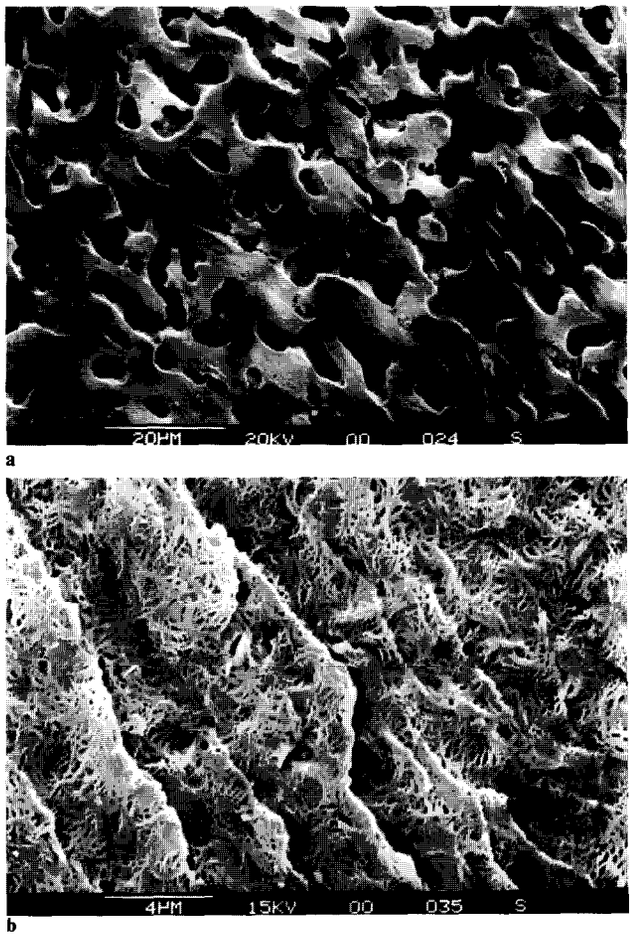

Figure 9 SEM micrographs of solvent-etched blends: (a) with no added catalyst; (b) after the addition of catalyst during melt blending but before thermal cycling

between the crystalline and amorphous phases and quadratic in the volume fraction of crystals ϕ, giving $Q' = \phi(1-\phi)\langle\eta^2\rangle$. Values of Q' were calculated via Simpson's rule integration of the $I(q,t)q^2$ vs q curves between the experimental limits of the first and last reliable data points (i.e. from $q = 0.01$ to $0.18\ \text{Å}^{-1}$). Plots of Q' vs temperature for the PBT and the blend are shown in *Figures 8a* and *8b*, respectively. The Q' data for the PBT (*Figure 8a*) again shows the good reproducibility in melting and recrystallization behaviour achieved over four thermal cycles. The initial melting behaviour of the as-received PBT (cycle 1) reflects its different thermal history, but during all four cycles the PBT exhibits a rapid decrease in Q' due to melting at $T_m \approx 220°C$, and a corresponding increase in Q' at $T_c \approx 200°C$ as recrystallization occurs. In addition, the glass transition of the PBT is evident as a change in slope of the invariant curves at $T_g \approx 40°C$. In the absence of phase changes, this is due to the change in slope of the expansion coefficient of the amorphous phase, c.f. the crystalline phase. The Q' data for the blend (*Figure 8b*) illustrates well the effects of transesterification. The initial heating cycle of the blend (cycle 1) shows melting at $T_m \approx 215°C$, recrystallization at $T_c \approx 200°C$ and two glass transitions; a broad change in slope beginning at ≈60°C attributed to a PBT-rich phase, and a higher temperature transition at ≈150°C attributed to a PC-rich phase. However, over the next three thermal cycles the blend exhibits only one discernible glass transition, which shifts from ≈60°C to ≈90°C as a result of transesterification. Transesterification also has significant affects on melting and recrystallization behaviour. Thus, over the four thermal cycles the degree of crystallinity (indicated by the value of Q') is reduced, and the values of T_m and T_c are seen to decrease by approximately 20°C and 10°C, respectively.

The effect of transesterification on blend morphology is illustrated clearly in *Figure 9*, which shows SEM micrographs of solvent-etched blends with no added catalyst (*Figure 9a*), and after the addition of catalyst during melt blending but before thermal cycling (*Figure 9b*). The uncatalysed blend exhibits a relatively coarse bicontinuous morphology in which the PC-rich phase has a size-scale of between 5 and 10 μm, whereas the catalysed blend shows a much finer, sub-micron, bicontinuous morphology. As thermal cycling proceeds the morphology of the blend is not amenable to solvent etching, first becoming resistant to the solvent, then completely soluble. This change in solubility with

increasing transesterification has been ascribed[2] to the formation, at low degrees of reaction, of block copolyesters with reduced solubility followed, at higher degrees of reaction, by completely soluble statistical copolymers.

The significant decrease in phase size-scale between *Figures 9a* and *9b* may be ascribed to interfacial transesterification between the homopolymers in the melt, resulting in the formation of AB-copolymers which act to reduce interfacial tension between the immiscible phases and produce a finer structure[21]. Melt transesterification will also have a significant effect on the kinetic competition between the processes of phase dissolution and PBT crystallization, which initiate as the melt is cooled below $T_S(\approx 200°C)$ and $T_m(\approx 220°C)$, respectively. In uncatalysed blends, crystallization is by far the quicker process and rapid solidification of the PBT-rich phase will limit phase dissolution to the interfacial regions. However, the much finer morphology which results from interfacial reaction will increase interfacial area within the blend, allowing phase dissolution to compete with crystallization and produce a significant volume of phase-mixed interphase material. As extensive transesterification also reduces the propensity of PBT to crystallize, eventually the 'blend' will be transformed into an amorphous, homogeneous mixture comprising homopolymers and various AB-type copolymers[12]. This scenario is consistent with the results obtained in this study, particularly the d.s.c. and SAXS invariant data (*Figures 2* and *8b*, respectively). These data show a progressive reduction in crystallinity with increasing transesterification and the development of a distinct mixed-phase glass transition at ~90°C.

SUMMARY AND CONCLUSIONS

The crystallization behaviour of pure PBT and a 50/50 PC–PBT blend with added transesterification catalyst were studied using d.s.c. and simultaneous synchrotron SAXS/WAXS/d.s.c. Both techniques showed pure PBT to exhibit highly reproducible crystallization behaviour during repeated thermal cycling between 30 and 250°C. In comparison, SAXS data showed the presence of PC in the blend to significantly retard the crystallization of the PBT, particularly at temperatures <160°C.

Interfacial transesterification between the homopolymers in the melt produced a significant retardation of PBT crystallization in the blend. Thus, WAXS data showed reduced peak intensities upon thermal cycling between 30 and 250°C. Whilst d.s.c. and SAXS invariant data displayed a progressive reduction in the degree of crystallinity and the melting (T_m) and crystallization (T_c) temperatures with increasing transesterification, and the development of a distinct mixed-phase glass transition at ~90°C which agrees well with the value of 86°C predicted by the Fox equation for a homogeneous material.

SEM showed transesterification to have a significant effect on blend morphology. Whereas an uncatalysed blend exhibited a relatively coarse (~10 μm) bicontinuous morphology, a catalysed blend had a much finer, submicron, bicontinuous morphology, resulting from the formation of AB-copolymers which reduce interfacial tension between the immiscible phases in the melt. A scenario was proposed in which the finer morphology resulting from interfacial reaction promoted phase dissolution as the blend cooled, at the expense of PBT crystallization. Eventually, transesterification will completely inhibit crystallization, and phase dissolution will transform the 'blend' into an amorphous, homogeneous mixture comprising homopolymers and various AB-type copolymers.

ACKNOWLEDGEMENTS

The authors thank EPSRC for beam time at Daresbury, and Ernie Komanschek for assistance with data collection. The kind donation of the reactants used in this study from Bayer and Du Pont is also gratefully acknowledged.

REFERENCES

1 Wahrmund, D. C., Paul, D. R. and Barlow, J. W. *J. Appl. Polym. Sci.* 1978, **22,** 2155
2 Devaux, J., Godard, P. and Mercier, J. P. *Polym. Eng. Sci.* 1982, **22,** 229
3 Birley, A. W. and Chen, X. Y. *Br. Polym. J.* 1984, **16,** 77
4 Birley, A. W. and Chen, X. Y. *Br. Polym. J.* 1985, **17,** 297
5 Hobbs, S. Y., Groshans, V. L., Dekkers, M. E. J. and Shultz A. R. *Polym. Bull.* 1987, **17,** 335
6 Delimoy, D., Bailly, C., Devaux, J. and Legras, R. *Polym. Eng. Sci.* 1988, **28,** 104
7 Kim, W. N. and Burns, C. M., *Makromol. Chem.* 1989, **190,** 661
8 Dekkers, M. E. J., Hobbs, S. Y., Bruker, I. and Watkins, V. H. *Polym. Eng. Sci.* 1990, **30,** 1628
9 Joyce, R. P. and Berzinis, A. P., 'Compalloy '91', Schotland Business Research Inc., Princeton, NJ, p. 65
10 Pompe, G., Meyer, E., Komber, H. and Hamann, H. *Thermochim. Acta* 1991, **187,** 185
11 Okamoto, M. and Inoue, T. *Polymer* 1994, **35,** 257
12 Wilkinson, A. N., Cole, D. and Tattum, S. B. *Polym. Bull.* 1995, **35,** 751
13 Delimoy, D., Goffaux, B., Devaux, J. and Legras, R. *Polymer* 1995, **36,** 3255
14 Kumaki, J. and Hashimoto, T. *Macromolecules* 1986, **19,** 763
15 Okamoto, N., Shiomi, K. and Inoue, T. *Polymer* 1995, **36,** 87
16 Jadhay, J. Y. and Kantor, S. W. in 'Encyclopaedia Polymer Science & Engineering', 2nd Edn, Vol. 12, John Wiley, New York, p. 217
17 Pilati, F., Manaresi, P., Fortunato, B., Munari, A. and Monari, P. *Polymer* 1983, **24,** 1479
18 Bras, W., Derbyshire, G. E., Devine, A., Clarke, S. M., Cooke, J., Komanscheck, B. U. and Ryan, A. J. *J. Appl. Cryst.* 1995, **28,** 26
19 Bras, W., Derbyshire, G. E., Ryan, A. J., Mant, G. R., Felton, A., Lewis, R. A., Hall, C. J. and Greaves, G. N. *Nucl. Instr. Meth. Phys. Res.* 1993, **A326,** 587
20 Barham, P. in 'Materials Science & Technology: A Comprehensive Treatment' (Eds R. W. Cahan, P. Haasen and E. J. Kramer), Vol. 12 (Vol. Ed. E. L. Thomas), VCH Pub., Weilheim, 1993, p. 138
21 Elmendorp, J. J. in 'Mixing in Polymer Processing' (Ed. C. Rauwendaal), Marcel Dekker, New York, 1990, p. 17